Published in final edited form as:
Dev Biol. 2011 May 15; 353(2): 242–258. doi:10.1016/j.ydbio.2011.02.031.

Six1 transcription factor is critical for coordination of epithelial, mesenchymal and vascular morphogenesis in the mammalian lung

Ahmed HK El-Hashash[1,*], **Denise Al Alam**[1], **Gianluca Turcatel**[1], **Orquidea Rogers**[1], **Sean Li**[2], **Saverio Bellusci**[1], and **David Warburton**[1,*]

[1] Developmental Biology and Regenerative Medicine Program, Saban Research Institute, Childrens Hospital Los Angeles, Keck School of Medicine of University of Southern California, 4650 Sunset Boulevard MS35, Los Angeles, CA 90027, USA

[2] Children's Hospital Boston, Harvard Medical School, USA

Abstract

Six1 is a member of the six-homeodomain family of transcription factors. Six1 is expressed in multiple embryonic cell types and plays important roles in proliferation, differentiation and survival of precursor cells of different organs, yet its function during lung development was hitherto unknown. Herein we show that *Six1*$^{-/-}$ lungs are severely hypoplastic with greatly reduced epithelial branching and increased mesenchymal cellularity. Six1 is expressed at the distal epithelial tips of branching tubules as well as in the surrounding distal mesenchyme. *Six1*$^{-/-}$ lung epithelial cells show increased expression of differentiation markers, but loss of progenitor cell markers. *Six1* overexpression in MLE15 lung epithelial cells in vitro inhibited cell differentiation, but increases the expression of progenitor cell markers. In addition, *Six1*$^{-/-}$ embryos and newborn mice exhibit mesenchymal overproliferation, decreased *Fgf10* expression and severe defects in the smooth muscle component of the bronchi and major pulmonary vessels. These defects lead to rupture of major vessels in mutant lungs after birth. Treatment of *Six1*$^{-/-}$ epithelial explants in culture with recombinant Fgf10 protein restores epithelial branching. As Shh expression is abnormally increased in *Six1*$^{-/-}$ lungs, we also treated mutant mesenchymal explants with recombinant Shh protein and found that these explants were competent to respond to Shh and continued to grow in culture. Furthermore, inhibition of Shh signaling with cyclopamine stimulated *Six1*$^{-/-}$ lungs to grow and branch in culture. This study provides the first evidence for the requirement of *Six1* in coordinating Shh-Fgf10 signaling in embryonic lung to ensure proper levels of proliferation and differentiation along the proximodistal axis of epithelial, mesenchymal and endothelial cells. These findings uncover novel and essential functions for *Six1* as a critical coordinator of Shh- Fgf10 signaling during embryonic lung development. We propose that *Six1* is hence critical for coordination of proper lung epithelial, mesenchymal and vascular development.

*Corresponding author: David Warburton, OBE, DSc, MD, MMM, FRCP, FRCS, FRCPCH, Developmental Biology, Regenerative Medicine and Surgery Program, Saban Research Institute, Children's Hospital Los Angeles, Keck School of Medicine and School of Dentistry, 4661 Sunset Boulevard MS 35, Los Angeles, California 90027, USA. Telephone: 323-361-5422, Fax: 323-361-3613, dwarburton@chla.usc.edu (D.Warburton), aelhashash@chla.usc.edu (A. El-Hashash).

Keywords

lung development; Six1; proliferation; differentiation; Shh; Fgf10

INTRODUCTION

Mammalian lung development is initiated by the formation of two primary epithelial buds, which arise from the laryngotracheal groove in the ventral floor of the primitive foregut endoderm and extend into the surrounding splanchnic mesenchyme. These buds undergo stereotypic rounds of branching and outgrowth to give rise to a tree-like respiratory organ, which contains different specialized epithelial cell types organized along the proximodistal axis (Cardoso, 2000; Metzger et al, 2009; Warburton et al., 2000, 2008, 2010). Controlled and rapid proliferation of lung epithelial progenitors, in association with the outgrowth and branching of the epithelial tubes, is essential for producing an alveolar gas diffusion surface sufficient to sustain extra-uterine life. The undifferentiated epithelial cells leave the progenitor pool to give rise first to lineage-committed precursor cells and eventually to fully differentiated cell lineages (Cardoso and Lü, 2006; Rawlins and Hogan, 2006). Disruption of normal lung developmental processes can result in neonatal respiratory failure or distress (i.e. pulmonary hypoplasia, a hallmark of congenital lung diseases) if lung formation is severely affected or susceptibility to lung diseases during later life if milder changes occur in the developing lung (Warburton et al., 2006).

Normal lung morphogenesis and patterning depend critically on interactive signaling between the endodermal epithelium and mesenchyme derived from splanchnic mesoderm. The pulmonary mesenchyme gives rise to several different cell types, including smooth muscle of the upper airways during branching morphogenesis. Moreover, the mesenchyme produces many important growth factors and signaling molecules required for airway epithelial branching and development, e.g. members of the fibroblast growth factor (Fgf) family (reviewed by Warburton et al., 2000, 2005, Morrisey and Hogan, 2010). In turn, the epithelium produces signaling molecules essential for mesenchymal proliferation and differentiation including sonic hedgehog (Shh) and bone morphogenetic protein 4 (BMP4) (Bellusci et al., 1996, 1997a,b; Litingtung et al., 1998; Pepicelli et al., 1998).

The sine oculis (SIX) proteins belong to a family of six homeodomain transcription factors, which are homologues of *Drosophila sine oculis*. In mammals, *Six* (*Six1–6*) genes and *Eya* are co-expressed and exhibit synergistic genetic interactions to regulate the development of multiple organs by controlling cell cycle regulators and inhibition of apoptosis (Kawakami, et al., 2000, Xu et al., 1997b; Ford et al., 1998; Coletta et al., 2004). In addition, *Six1* and *Six4* play important roles in the formation of various organs such as olfactory epithelium, cranial ganglia, inner ear, kidney, skeletal muscle and skeleton (reviewed by Kawakami et al., 2000; Kumar, 2009). *Six1*$^{-/-}$ mouse embryos have defects in the proliferation and survival of the precursor cells of multiple organs, and die at birth (Xu et al., 2002; Laclef et al., 2003; Li et al., 2003). Mutations in the Six protein family (Six1 or Six5) or in Eya1 protein are responsible for Branchio-Oto-Renal syndrome in humans (Abdelhak et al., 1997; Ruf et al., 2004; Hoskins, et al., 2007; Krug et al., 2010).

The *Eya1* gene encodes a transcriptional co-activator that acts with *Six1* to control the development of different organs (Zou et al., 2004, 2006a; Grifone et al., 2004). We recently reported a severely hypoplastic lung phenotype in *Eya1*$^{-/-}$ embryos (El-Hashash et al., 2011). Yet the specific functions of *Six1* in lung development are unknown.

Herein, we found that *Six1* deletion causes severe lung hypoplasia, increased epithelial differentiation, pulmonary smooth muscle defects and disruption of Shh-Fgf10 signalling, which suggest that *Six1* is necessary for proper coordination of epithelial, mesenchymal and endothelial tissues during lung development.

MATERIALS AND METHODS

Animals and genotyping

Six1 knockout (KO) mice on the 129 background, $Fgf10^{LacZ/+}$, and $Fgf10^{LacZ/-}$ hypomorph mice have been published previously (Kelly et al., 2001; Laclef et al., 2003; Xu et al., 2002, 2003; Mailleux et al., 2005). Genotyping of mice and embryos was performed as previously described (Kelly et al., 2001; Laclef et al., 2003; Xu et al., 2002, Perl et al., 2002). Wildtype littermates were used as controls.

Phenotype analysis, in situ hybridization (ISH) and Real-time PCR

Histological staining and ISH using *Six1* probe were performed as previously described (Xu et al., 1997a; De Langhe et al., 2006). Real-time PCR and semi-Quantitative PCR were performed in triplicate as described before (Del Moral et al. 2006a,b). PCR primers used in this study were described in Table 1 in the Supplemental Data.

Immunohistochemical/X- gal staining and BrdU labeling

Immunohistochemical/X-gal staining on paraffin sections or fixed MLE-15 cells and bromodeoxyuridine (BrdU) labeling were performed using standard protocols as described (Tefft et al., 2005; El-Hashash et al., 2005; Del Moral et al. 2006a,b). Antibodies used in this study are described in Table 2 in the Supplemental Data. Staining was performed in triplicate. For all immunohistochemistry, mutant sections were mounted on the same slides of wildtype control sections and processed for antibody staining under the same conditions.

Isolated epithelial and mesenchymal explant cultures

Lungs from E12.5 embryos were treated with dispase (BD Biosciences) for 5 min at 4 °C and then transferred to Dulbecco's Modified Eagle's Medium: Nutrient Mixture F-12 (DMEM:F12) with 10% fetal bovine serum (FBS; Invitrogen) to block the enzymatic reaction. The epithelial buds were separated from the mesenchyme, embedded in 200 μl of Matrigel diluted 1:1 with DMEM:F12 serum-free media containing 250 ng/ml recombinant Fgf10 (R & D Systems), and then grown in culture as described (Carraro et al., 2009). Isolated mesenchymal explants were grown on Matrigel and treated with 500 ng/ml recombinant Shh (R & D Systems) as previously described (Weaver et al., 2003; Del Moral et al., 2006a).

Whole-lung culture and treatment with cyclopamine

Embryonic lungs were removed at E11.5 grown in culture and treated with cyclopamine as described (Mailleux et al., 2005). Briefly, lungs were placed on Nuclepore filters in 30 μl of a 1:1 mixture of Matrigel and culture medium (DMEM/F12 medium containing 0.1% heat-inactivated fetal bovine serum and penicillin/streptomycin) and kept for 30 minutes at 37°C. After Matrigel polymerization, these filters were laid on the surface of 500μl culture medium containing cyclopamine (TRC Biomedical Research Chemicals, Canada) in Nunclon dishes. Concentrations of 2, 5 and 10 μmol/l cyclopamine were tested and cyclopamine proved toxic at 10 μmol/l as previously described (Yao et al., 2002; Mailleux et al., 2005). Lungs were cultured for 2 days in the presence of cyclopamine and then fixed in 4% PFA.

Cell culture and transfection

Lung epithelial cells MLE15, a gift from Jeffrey Whitsett (Cincinnati University), were grown in culture and treated as well as processed for transfection as described (Tefft et al., 2002). Briefly, for transfection MLE15 cells were seeded in eight chamber slides (BD Biosciences) at 50 % confluency. The next day they were transfected with 200 ng of expression vector for mouse *Six1* or a luciferase-expressing vector (control) using lipofectamine LTX (Invitrogen). Fresh medium was added 6 hours later. Cells were fixed with 4%PFA three days after transfection as above. We used an expression vector encoding a VP16 fusion protein and the transfection efficiency was monitored by fluorescence staining using anti-VP16 antibody.

Data and statistical analysis

Data are presented as means ± SD. Statistical significance between wildtype control and mutant lungs was calculated using Student's *t*-test. For counting PHH3-, Caspase-3, SP-B, SP-C or CC10- positive cells, labeled epithelial or mesenchymal cells and total cell number per section were counted. Three random fields were chosen (200–350 cells per field) from three different embryos of each indicated genotype. The percent of labeled cells to the total cell number was reported. Analyses were done using GraphPad Prism software (GraphPad Software, Inc., San Diego, http://www.graphpad.com). Densitometry analysis was produced by the software Image J.

RESULTS

Six1 is expressed in distal epithelium and mesenchyme of embryonic lung

Semi-quantitative RT-PCR analysis demonstrated that levels of *Six1* transcripts are highest during initiation and branching phases of lung development (E9.5–E11.5 and E11.5–E17.5; respectively in mouse) then decline significantly during the differentiation phase (after E18.5; Fig. 1A). *Six1* transcripts were detected in the lung bud from E9.5 (Fig. 1D,E) and also in the pharyngeal region and ear (Fig. 1D,E and Xu et al., 2002; Zheng et al., 2003). Six1 protein was more specifically expressed in distal lung mesenchymal and epithelial cells from around E12.5 to E18.5 (Fig. 1B,C,F,G,K,L). The specificity of Six1 antibody was confirmed by Western blotting of lung proteins where it detected a proper expected protein band of 32 kDa, which corresponds to the size of Six1 protein (data not shown).

It has been reported that *LacZ* expression in $Fgf10^{LacZ/+}$ mouse lung can be used as a reporter for *Fgf10* expression (Mailleux et al., 2005). Interestingly, X-gal staining of E14 $Fgf10^{LacZ/+}$ lungs and Six1 antibody staining show striking similarity in the focal expression pattern of *Fgf10* and Six1 in the distal mesenchyme adjacent to distal tips of branching tubules (Fig. 1H,I). Double staining of X-gal-stained $Fgf10^{LacZ/+}$ lungs with Six1 antibody further confirmed the expression of both Six1 and *Fgf10* in the distal mesenchyme (Fig. 1J).

Six1$^{-/-}$ embryos die quickly after birth due to respiratory failure and display severe lung hypoplasia

The *Six1* mutant embryos die quickly after birth, have defects in several organs and are relatively smaller in size than wildtype littermates (Xu et al., 2002; Laclef et al., 2003). Observation of the newborn pups revealed that the 25% of them, which were genotyped as $Six1^{-/-}$ mice, gasped for breath and appeared cyanotic. When compared with the lungs of wildtype littermates the lungs of E14.5 and E18.5 $Six1^{-/-}$ embryos were significantly smaller in appearance (Fig. 2A,D) but had normal initial lobation. No Six1 protein expression was evident in $Six1^{-/-}$ lungs (Figure S1 G in the Supplemental Data), and both histological and marker analyses showed that heterozygous lungs have no apparent lung

defects in mouse embryos, which continue to grow, breathe and breed normally after birth (data not shown).

Histological analysis of hematoxylin-eosin-stained sections from wildtype versus *Six1*$^{-/-}$ mice showed that, as expected, E18.5 wildtype lungs were properly fluid inflated (Fig. 2D,E,I). However, *Six1*$^{-/-}$ lungs were not fluid inflated and had a smaller, collapsed appearance (Fig. 2D,F,J). This severe lung phenotype was also observed in E14.5 *Six1*$^{-/-}$ embryos (Fig. 2A–C, G,H). Furthermore, *Six1*$^{-/-}$ lungs were severely hypoplastic: morphogenesis of E18.5 mutant lungs appeared to be arrested in the pseudoglandular stage of development (Fig. 2E,F,I,J). *Six1*$^{-/-}$ lungs also showed an increase in the ratio of interstitial mesenchyme to epithelial tubules, while expansion of epithelial tubules did occur, but was greatly reduced versus wildtype lungs (compare Fig. 2F,J with E,I). Also, primitive pre-alveoli were greatly reduced in *Six1*$^{-/-}$ lungs (Fig. 2J), with different degrees of severity (compare Fig. 2F,J with Fig. 4G an Fig. 2C,H with Fig. 6B,F). Thus, E18.5 *Six1*$^{-/-}$ mutant lungs depicted the histopathological features of pulmonary hypoplasia: small sized lungs, greatly reduced branching morphogenesis, narrow bronchi, arrested expansion of epithelial tubules and dense mesenchymal cellularity as well as apparent failure of normal lung maturation (interstitial condensation), which should occur in late lung development (Fig. 2F,J). Moreover, *Six1*$^{-/-}$ mice exhibited congestion of large blood vessels (Fig. 8B,F). These data suggest that *Six1* $^{-/-}$ mice die quickly after birth because of respiratory failure and the lungs of these mice display several severe hypoplastic defects, including lack of inflation and pulmonary hemorrhage.

Next, to determine the timing of onset of phenotypic abnormalities during *Six1*$^{-/-}$ lung organogenesis we examined lung development at E10–10.5 (Figure S1 in the Supplemental Data). In *Six1*$^{-/-}$ lungs, very early branching and development were comparable with control littermate lungs, wherein two primary buds arose in the ventrolateral foregut at E9.5 and underwent stereotypic rounds of branching and outgrowth in order to give rise to an early tree like organ (Figs. S1A–B, D–E). However, both whole-mount and sections at E13–14.5 revealed that lung hypoplasia was noticeable as early as E13–13.5 of development and was more severe from E14.5 (Fig. 2A–C,G,H and data not shown for E13–13.5). Consequently, E13–13.5, E14.5 and E18.5 were used as the developmental stage of choice to analyze the *Six1*$^{-/-}$ lung phenotype in this study. Taken together, these data suggest that *Six1* is unlikely to be involved directly in primary lung bud induction and is thus not required for the initiation of early mammalian lung organogenesis. Thus the major impact of *Six1* deletion is on lung branching morphogenesis subsequent to the first round(s) of domain branching.

Changes of cell proliferation of both epithelial and mesenchymal tissues in *Six1*$^{-/-}$ lungs

Our observations about the abnormal mesenchymal phenotype of the *Six1*$^{-/-}$ lungs further suggest that *Six1* abrogation results in increased mesenchymal cell proliferation and/or cell survival. To test this hypothesis, we stained for Phospho-histone 3 (PHH3), which is an immunomarker specific for cells undergoing mitoses and is a reliable method for identifying mitotic figures and determining mitotic index (Colman et al., 2006). When lung hypoplasia became noticeable at E13.5, PHH3 staining showed a marked increase of PHH3-positives cells in the mutant mesenchyme, but a clear decrease in epithelial cell proliferation in *Six1*$^{-/-}$ lungs (Fig. 3C,D). At E14.5, a stage when the lung phenotype became severe, PHH3 staining demonstrated a 1.7-fold decrease in the number of mitotic cells in the epithelium, but a 1.6-fold increase in the number of mitotic cells per total cell number in the mesenchyme of *Six1*$^{-/-}$ lungs (55.0±2.2% versus 31.0±3.0% for the epithelium, and 26.0±2.0% versus 43.0±2.8 for the mesenchyme, n=3, p< 0.05; Fig. 3A,B,G). On the contrary, cell proliferation analysis using PHH3 staining as a proliferation marker at E12.5

showed that cell proliferation appears comparable for both epithelial and mesenchymal compartments between *Six1*$^{-/-}$ and control lungs (Fig. 3J,K).

At later stages of development, cell proliferation was further examined by exposing E18.5 embryos in utero to BrdU for 1 hour. The relative proportion of cells that had entered or passed through S phase was then determined by immunocytochemistry of lung sections, which showed a dramatic increase of BrdU-positive proliferative cells in *Six1*$^{-/-}$ lungs (Fig. 3E,F). Caspase-3 staining showed no obvious increase in cell death in E13.5, E14.5 and E18.5 mutant lungs (Fig. 3H,I, and data not shown). Together, these data suggest that *Six1* is a critical regulator of cell proliferation in the embryonic lung.

Six1 deletion increases epithelial differentiation in embryonic lungs

Lung epithelial cells differentiate during mid to late gestation of embryonic development, resulting in distinct cell lineages being distributed along a proximodistal axis (Warburton et al., 2000, 2005, 2008). Since *Six1* negatively regulates cell differentiation in other cell types (e.g. placodal neuronal progenitors; Schlosser et al., 2008), we next determined whether lung epithelial cell differentiation had occurred properly after *Six1* deletion by examining the expression of markers for proximal (CC10) and distal (SP-A, SP-B, and SP-C) epithelial differentiation at E18.5. Transcripts for these differentiation markers were increased in E18.5 *Six1*$^{-/-}$ lungs compared to wildtype littermates (example is shown for *SP-B* in Fig. 4J).

During lung development, late differentiation markers SP-C and SP-B are expressed in alveolar type II (AEC-2) cells of the distal airways, whereas CC10 expression is normally confined to non-ciliated Clara epithelial cells of the proximal airways in wildtype lungs (Fig. 4A,F,K). Immunohistochemistry of mutant and control sections, which were mounted on the same slides and developed for staining under the same conditions, showed an apparent increase in the relative number of epithelial cells positive for SP-B, SP-C and CC10 proteins in *Six1*$^{-/-}$ lungs (Fig. 4,B,G,L). In particular, the percent of cells positive for SP-C showed an increase, which ranged from 1.7–2.4 fold, in *Six1*$^{-/-}$ mutant versus control lungs (positive cells were counted in 200× per field, *n=3*; Fig. 4E). A similar increase was shown also for SP-B- or CC10-positive cells (positive cells were counts in 200× per field, $n = 3$, $p < 0.05$; Fig. 4E). Interestingly, while more cells are expressing these differentiation markers, the level of protein expression is not increased on a per cell basis in *Eya1*$^{-/-}$ lungs compared to control lungs (compare Fig. 4D,I,N with C,H,M). The increase of both SP-B and SP-C expression was also evident in *Six1*$^{-/-}$ lungs early during the pseudoglandular stage at E14.5 (Fig. 5B,E).

Next, we further investigated *Six1* effects on lung epithelial cell differentiation in vitro using MLE15 lung epithelial cells, which express endogenous Six1 as well as different epithelial differentiation and progenitor cell markers (Figs. 5C, 6C,D,G,H and data not shown). As shown in Fig. 5C, MLE15 cells transfected with *Six1* expression vector showed a decrease in the expression levels of several lung epithelial differentiation markers, which further supports the inhibitory function of *Six1* on lung epithelial differentiation.

Distal epithelial progenitors are severely reduced in the *Six1*$^{-/-}$ embryonic lungs

Six1 is a critical regulator of embryonic cell maintenance/survival, and *Six1*$^{-/-}$ mouse embryos have defects in the proliferation and survival of the progenitors of several organs (Xu et al., 2002; Laclef et al., 2003; Li et al., 2003). Therefore, we next determined the effects of *Six1* on lung epithelial progenitors using antibodies against Sox9, Id2 and N-myc, which were highly expressed in lung distal epithelial progenitors (Fig. 6A,E,I; Okubo et al., 2005; Rawlins, 2008), wherein Six1 was also highly expressed (Fig. 1B,C). Sox9

transcription factor was specifically expressed in the distal epithelial progenitors from E11.5 to E16.5 (Figs. 6A, 7A,B) and becomes undetectable by E18.5 (Liu and Hogan, 2002). In *Six1*$^{-/-}$ lungs, signals of Sox9, Id2 and N-myc transcription factors were markedly reduced at E13.5 (Fig. 7D,H and data not shown), a stage when lung hypoplasia became noticeable, and prematurely abolished in the distal epithelium at E14.5 (Fig. 6B,F,J). In addition, real-time PCR analysis of E14.5 mutant lungs showed markedly reduced expression of *Sox9* at the gene levels (Fig. 6K).

Next, to determine whether normal embryonic epithelial progenitors have ever formed in *Six1*$^{-/-}$ lungs, we stained for progenitor cell markers at early embryonic stages. As shown in Fig. 7, *Six1*$^{-/-}$ distal epithelial tips stained positively for Sox9 and Id2 and no apparent change was observed in the expression levels of these markers at E12–12.5 compared to wildtype littermates (Fig. 7A,C,E,G). This suggests that distal epithelial progenitors have formed normally but become rapidly depleted at the pseudoglandular phase of *Six1*$^{-/-}$ lungs. Therefore, *Six1* must be a critical regulator of the maintenance of lung epithelial progenitors and of the correct expression of progenitor cell markers. This hypothesis was further supported by our in vitro studies using MLE15 epithelial cells. Thus, *Six1* overexpression in MLE15 lung epithelial cells stimulated a marked increase in Sox9 and Id2-expressing cells as well as increased mitotic cells in culture (Fig. 6C,D,G,H,L).

Taken together, these data suggest that *Six1*$^{-/-}$ embryos display lung epithelial defects that correlate with increased epithelial differentiation and decreased epithelial progenitors.

Six1$^{-/-}$ embryos display pulmonary vascular defects

At E18.5 and at birth (P0), close examination of *Six1*$^{-/-}$ embryos showed congestion of the large pulmonary vessels, suggesting a pulmonary vascular defect in these embryos (Figs. 8A,B,C,D). Notably, this congestion of blood vessels was not observed in any other region of the embryos or neonates (data not shown), suggesting a specific defect in the lung vasculature. Moreover, no apparent change in the number of PHH3-positive mitotic smooth muscle or endothelial cells was observed in the large pulmonary blood vessels (Fig. 8E,F). In addition, caspase-3-positive apoptotic cells were few and did not significantly change within the pulmonary vasculature of *Six1*$^{-/-}$ and control lungs (Fig. 8I).

In addition, many *Six1*$^{-/-}$ pulmonary vessels were either small/collapsed (compare Fig. 9A with 9B,D) or showing rupture of the vascular smooth muscle wall, which was thin (one layer; compare Fig. 9C and 9D) with herniation of the endothelial lining (Fig. 9B, and data not shown). These results showed that *Six1*$^{-/-}$ lungs of late stage embryos and neonates exhibited vascular smooth muscle-specific defects and congested blood vessels. Thus, in *Six1*$^{-/-}$ embryos weakened pulmonary blood vessels could rupture at birth, possibly due to the increased pulmonary blood flow or internal mechanical strain on the lungs, which occurs in association with the transition to air breathing at birth, particularly when the lung is dysplastic.

Severe reduction of vascular and bronchial smooth muscle α-actin expression in *Six1*$^{-/-}$ lungs

Our hypothesis is that the weakened and congested state of the pulmonary blood vessels observed in the lungs of *Six1*$^{-/-}$ embryos/neonates is largely due to defects in vascular smooth muscle cell (VSMC) differentiation. To test this hypothesis, we determine whether smooth muscle had differentiated properly in *Six1*$^{-/-}$ embryos/neonates by immunostaining for smooth muscle α-actin (α–SMA), which is normally mainly detected in cells surrounding blood vessels and the conducting airways (Mitchell et al., 1990; Low and White, 1998). At E18.5, differentiated smooth muscle cells are normally seen surrounding all the major

pulmonary vasculature and the large upper bronchial airways in late development in control wildtype lungs (Fig. 9A,E). In contrast, most of the blood vessels of E18.5 *Six1*$^{-/-}$ lungs contained noticeably thin and less differentiated smooth muscle with frank breaches in the vessel wall, while some had almost undetectable smooth muscle α-actin staining (Fig. 9B,D). Similarly, α–SMA expression was hardly detectable in *Six1*$^{-/-}$ bronchial smooth muscles (Fig. 9F), although muscle cells appeared to morphologically exist with their characteristic spindle shape (Nie et al., 2010) surrounding pulmonary vasculature and large bronchial airways (Fig. 9D,H), as compared to control lungs (Fig. 9C,G). These defects in vascular and bronchial smooth muscle were not correlated with increased smooth muscle cell death in E18.5 *Six1*$^{-/-}$ lungs, as indicated by caspase-3 staining of blood vessels and bronchi (Fig. 8I). These data suggest that *Six1* is critical for the differentiation of both pulmonary bronchial and vascular smooth muscle and hence the integrity of the lung vasculature during lung development.

We next stained *Six1*$^{-/-}$ lungs with an antibody to platelet endothelial adhesion molecule (PECAM) to determine whether the smaller vessels in the lung, which lack vascular smooth muscle, were affected in *Six1*$^{-/-}$ embryos. Signals for PECAM, a marker for endothelial cells, were observed in E18.5 *Six1*$^{-/-}$ and control lungs (Fig. 9I,J, $n = 3$ for each genotype), suggesting that vascular endothelium and capillary network are formed in *Six1*$^{-/-}$ lungs.

Increased Shh signaling activity, but decreased *Fgf10* expression in *Six1*$^{-/-}$ lungs

To determine the possible mechanisms by which absence of *Six1* results in the phenotype described above, we examined the expression of Shh. Two lines of reasoning led us to examine Shh expression and its relationship with *Six1* in the lung. Firstly, similar to Six1 (Fig. 1), *Shh* expression is most intense in the distal epithelial tips of the lung and is downregulated during the differentiation phase of murine lung development (from E16.5; Urase et al., 1996; Bellusci et al., 1997b). Secondly, ectopic lung-specific overexpression of *Shh* from an *Sp-c* promoter/enhancer construct (*Sp-c:Shh*) in transgenic mice yields a phenotype that is very similar to the *Six1*$^{-/-}$ lung phenotype (see above; and Bellusci et al., 1997b). In addition, both real-time PCR and immunohistochemistry showed a dramatic increase (5-fold) in *Shh* gene expression in E18–18.5 *Six1*$^{-/-}$ versus control lungs (Fig. 10L) and in Shh protein expression in both E14.5 and E18.5 *Six1*$^{-/-}$ lungs (Fig. 10B,D versus A,C). Thus Shh expression continued to increase at both gene and protein levels in *Six1*$^{-/-}$ lungs after E16.5, a time point where *Shh* expression should start to decrease progressively in wildtype lungs (Bellusci et al., 1997b), until birth (Fig. 10B,D,L and data not shown at P0, $n = 3$ for each genotype).

Hedgehog signaling competence is reflected by measuring Shh receptor patched-1 (Ptc-1) and Gli1 expression levels, which are expressed in lung distal mesenchyme and are mediators of Shh activity (Grindley et al., 1997, Lees et al., 2005; Madison et al., 2005). Therefore, we next investigated the expression of Ptc-1 and Gli1 (Fig. 10E–H, J–K). Beginning around E16.5 of embryonic development, *Shh*, *Ptc* and *Gli1/Gli2* RNA levels are normally declining in wildtype lungs, and *Shh* overexpression results in increased levels of both *Ptc* and *Gli* mRNAs in the lung (Grindley et al., 1997; Bellusci et al., 1997b). In *Six1*$^{-/-}$ lungs, the expression levels of Ptc-1 and Gli proteins were dramatically increased in the mesenchyme at E14.5 and E18.5 compared to wildtype control lungs (Fig. 10F,H,K versus E,G,J). Together, these data suggest that *Six1* absence causes a significant increase in Shh expression and activity and that *Six1* is necessary for normal down-regulation of Shh signaling activity starting from E16.5 in the lung.

Since ectopic *Shh* overexpression inhibits *Fgf10* expression in the lung (Bellusci et al., 1997b), we next examined changes in *Fgf10* expression in mutant versus wildtype lungs. As shown in Fig. 10 L, *Fgf10* expression was markedly decreased in parallel to increased *Shh*

expression levels in *Six1*$^{-/-}$ lungs, as measured by real-time PCR (Fig. 10L). This suggests that *Six1* acts upstream of Fgf10 signaling, which is active in the mesenchyme at the very distal tips of branching tubules and is critical for lung bud formation and epithelial branching (Bellusci et al., 1997a,b). This conclusion was further supported by analysis of *Six1* expression in *Fgf10* hypomorphic lungs where no change in *Six1* expression was apparently evident at different stages of lung development (example is shown in Fig. 10I).

Shh protein stimulates *Six1*$^{-/-}$ mesenchymal growth, while Fgf10 protein induces *Six1*$^{-/-}$ epithelial branching morphogenesis in culture

Having established that Shh-Fgf10 signaling is altered in *Six1*$^{-/-}$ lungs, we next investigated whether Shh and Fgf10 protens affect *Six1*$^{-/-}$ lungs in vitro. To test this possibility, the distal mesenchyme and epithelium of E12.5 *Six1*$^{-/-}$ lungs were separated and individually cultured in Matrigel-based three-dimensional scaffold in the presence or absence of Shh or Fgf10 recombinant protein, respectively. As shown in Fig. 11, all isolated mesenchymal explants from either control wildtype lungs (Fig. 11A,E; *n*= 8) or *Six1*$^{-/-}$ lungs (Fig. 11C,G; *n*= 8), which were cultured for 48 hr in control media, condensed and died. In cultures treated with 500 ng/ml Shh protein (Weaver et al., 2003; Li et al., 2005), a remarkable increase in the size of all tested control (Fig. 11B,F; *n*=8) and *Six1*$^{-/-}$ (Fig. 11D,H; *n*=8) mesenchymal explants was observed, associated with many elongated mesenchymal cells invading into the Matrigel at the periphery.

Next, we tested the hypothesis that excessive *Shh*-mediated reduction of *Fgf10* expression resulted in reduction of epithelial branching morphogenesis by using epithelial culture of *Six1*$^{-/-}$ lungs. E12.5 *Six1*$^{-/-}$ epithelial explants were grown for 48 hr in culture in Matrigel in the presence of 250 ng/ml Fgf10 (*n*=8). In the absence of Fgf10, neither the wildtype nor the *Six1*$^{-/-}$ lung isolated airways showed signs of branching and died (*n*=6; Fig. 11I,M,Q,K,O,S) as previously described for wildtype lungs (Bellusci et al., 1997a,b). But notably, addition of exogenous Fgf10 rescued *Six1*$^{-/-}$ branching defects so that most mutant epithelial explants (7 out of 8 explants) continued to grow and branch to form new branching tips in the presence of Fgf10 protein in a similar fashion to control explants (8 out of 8 explants grew) from early culture times (8–16hr of culture; Fig. 11L,P,T versus J,N,R). The inductive effect of Fgf10 protein on branching was even more pronounced after 24 hr of culture (data not shown). These data suggest that *Six1*$^{-/-}$ distal epithelial tip cells remain fully competent to respond to inductive signals from lung mesenchyme and that *Six1*$^{-/-}$ branching defects are therefore not an intrinsic property of the *Six1*$^{-/-}$ epithelium.

Cyclopamine inhibition of the Shh pathway induces *Six1*$^{-/-}$ lung growth in culture

To test the effect of inhibition of the biological effect of Shh signaling on *Six1*$^{-/-}$ lung growth and branching in vitro, we carried out cultures of whole lungs isolated at E12–E12.5 over a period of 42 hr in the presence or absence of the specific Shh antagonist, cyclopamine (Yao et al., 2002; Fig. 12). Without the addition of cyclopamine, all tested wildtype control lungs showed an increasing number of distal end buds (Fig. 12A,E,I), while all *Six1*$^{-/-}$ mutant lungs did not grow well in culture and showed a delay in their development compared to control lungs (Fig. 12C,G,K; *n*=9). By contrast, in the presence of 5 μmol/l cyclopamine a notable increase of lung size and epithelial branching after 42 hr of culture associated with a dilation of the distal epithelium was observed in all tested *Six1*$^{-/-}$ lungs (Fig. 12D,H,L; *n*=9) and control lungs (Fig. 12B,F,J). These data suggest that inhibition of Shh signaling activity can, at least partially, rescue *Six1*$^{-/-}$ lung developmental defects. This conclusion was further supported by developmental marker analyses at 26 hr of culture (Fig. 13). Thus, both Shh and SP-B expression levels was downregulated to control levels (Fig. 13A–C,G–I), while Sox9 expression and PHH-3 positive cells increased in mutant lungs treated with 5 μmol/l cyclopamine (Fig. 13D–F, J–M).

Taken together, our results provide the first direct evidence for the requirement of *Six1* in coordinating Shh-Fgf10 signaling during lung development and that the Six1-Shh-Fgf10 signaling pathway is therefore critical for lung epithelial branching morphogenesis.

DISCUSSION

We have demonstrated an important, seemingly complex role for Six1 transcription factor in a signaling network coordinating several different integrated processes required for correct lung development.

Six1 regulates both epithelial and mesenchymal cell proliferation in the embryonic lung

Our data demonstrate that *Six1* plays an essential role in proliferation of both the lung epithelium and mesenchyme. This observation is noticeable during the pseudoglandular phase where cell proliferation at distal epithelial tips that express Six1 is reduced from E13.5 onwards in *Six1*$^{-/-}$ lungs. In contrast, mesenchymal proliferation is somewhat unexpectedly greatly increased in the face of *Six1* deletion in *Six1*$^{-/-}$ lungs at E13.5 and later in development.

Six1 transcription factor plays critical roles in the regulation of precursor cell cycle and proliferation in different organs (Li et al., 2003; Kumar, 2009). Loss of *Six1* greatly reduces cell proliferation of otic epithelium (Zheng et al., 2003) and of both muscle and kidney (Li et al., 2003). Conversely, high levels of *Six1* expand the pool of proliferative neuronal progenitors (Schlosser et al., 2008). Thus, whereas lack of *Six1* expression in *Six1*$^{-/-}$ lung distal epithelium may account for reduced cell proliferation at the distal tips, the increased mesenchymal proliferation in *Six1*$^{-/-}$ lungs is less likely to be a direct effect of *Six1* deletion. Instead, *Six1* must act indirectly on mesenchymal proliferation by affecting other key regulators of mesenchymal cell proliferation such as Shh signaling, which regulates cell proliferation of lung mesenchyme (Litingtung et al., 1998; Pepicelli et al., 1998).

Six1 is essential for Shh expression and activity during lung development

In this current study we propose that the severe *Six1*$^{-/-}$ hypoplastic lung phenotype described herein (Fig. 2) may be explained by abnormal persistence of Shh expression/activity, occasioned by absence of *Six1* activity, for several reasons. Firstly, Shh acts as a mitogen for lung mesenchyme and thus controls epithelial branching indirectly during lung development (Bellusci et al., 1997b). Interestingly, embryonic *Six1*$^{-/-}$ lungs show increased mesenchymal cellularity with reduced branching and exhibit failure of interstitial condensation. The later is an important feature of prenatal fetal lung maturation, an abnormal phenotype that is most likely to be mediated through abnormally persistent high-level expression and activity of Shh (Bellusci et al., 1997b). Indeed, Shh expression and activity are high at E18.5 and at birth in *Six1*$^{-/-}$ lungs (i.e. after E16.5, a time point where *Shh* expression should start to decrease progressively in wildtype lungs (Bellusci et al., 1997b). Secondly, the phenotype of the *Shh* over-expressing transgenic lung bears striking similarities to the *Six1*$^{-/-}$ lung phenotype described herein (Fig. 2 and Bellusci et al., 1997b). Thirdly, both Six1 and Shh are highly expressed at distal epithelial tips of branching tubules (Fig. 1B,C, and Bellusci et al., 1997b) as well as being involved in controlling branching morphogenesis through regulation of mesenchymal development (Fig. 3, Bellusci et al., 1997b; Litingtung et al., 1998; Pepicelli et al., 1998).

Finally, our findings that *Six1*$^{-/-}$ lungs treated with the Shh-inhibitor cyclopamine continue to grow and branch in culture similar to wildtype lung (Figs. 12,13) provide strong confirmatory evidence for the negative modulatory effect of *Six1* on Shh signaling activity to ensure proper embryonic lung development. Moreover, since *Shh* null mice also have

pulmonary hypoplasia (Litingtung et al., 1998; Pepicelli et al., 1998), it is clear that levels of *Shh* expression must be tightly regulated in order for normal lung development to occur. Thus our findings are crucial for understanding how Shh expression/activity is indeed tightly regulated and for identifying *Six1* as a potential regulator of Shh expression and activity, which ensures appropriate mesenchymal/epithelial proliferation and differentiation in the embryonic lung. Our recent findings that deletion of *Eya1*, which acts as a transcriptional coactivator of *Six1* during the development of different organs (Jemc and Rebay, 2007), also results in an ectopic increase of Shh activity and a hypoplastic lung phenotype (El-Hashash et al., 2011) similar to the herein reported *Six1*$^{-/-}$ lung phenotype, further supports the importance of the Six1-Eya1 pathway as a potential key regulator of Shh expression level/activity in the lung.

The role of *Six1* in lung epithelial branching and differentiation

Lung induction involves the interplay between epithelial Shh and mesenchymal Fgf10. Our data show that *Six1*$^{-/-}$ embryonic lungs are characterized by a significant decrease in *Fgf10* expression, which is combined with increased *Shh* expression during the pseudoglandular stage and later in development (Fig. 10L). This suggests that *Six1* potentially promotes Fgf10 signaling pathway by negatively modulating Shh signaling, which in turn is a key inhibitor of Fgf10 signaling. This is internally consistent with the known function of Shh as a negative regulator of Fgf10 signaling to induce lung bud formation/epithelial branching (Bellusci et al., 1997a,b; Pepicelli et al, 1998).

It should be noted that *Six1* abrogation negatively impinges on lung branching morphogenesis subsequent to the first round(s) of domain branching (Fig. S1) somewhat similarly to *Shh*$^{-/-}$ lungs (Pepicelli et al, 1998). This occurs in parallel to increased Shh activity and reduced *Fgf10* expression in *Six1*$^{-/-}$ lungs. Thus, we propose that critical interactions between these three molecules occur in a novel Six1-Shh-Fgf10 pathway, which regulates subsequent rounds of epithelial branching. This conclusion is further supported by the findings that inhibiting Shh function in culture increases epithelial branching of *Six1*$^{-/-}$ lungs and treatment of *Six1*$^{-/-}$ epithelium in vitro with Fgf10 protein stimulates branching of the isolated mesenchyme-free airways (Figs. 11–13).

Other lines of evidence to support our novel hypothesis that *Six1* is a potential critical regulator of the Shh-controlled Fgf10 signaling in the lung come from knockout mice. Thus, similar to *Six1* functions reported herein, Fgf10 signaling is essential for the maintenance of epithelial progenitor cell proliferation (Ramasamy et al., 2007) and positively regulates the expression of epithelial progenitor marker Sox9 (Abler et al., 2009). In addition, Fgf10 signaling also inhibits differentiation of the lung epithelium (Nyeng et al., 2008) similar to *Six1* differentiation inhibitory functions (this study and Schlosser et al., 2008). Furthermore, both epithelial branching (Abler et al., 2009) and bronchial smooth muscle cells (Mailleux et al., 2005, Ramasamy et al., 2007) are severely defective in *Fgf10* hypomorphic or *Fgf10/Fgfr2b* inactivated lungs, which are very similar to the *Six1*$^{-/-}$ lung phenotype (Figs. 2, 9). Moreover, *Six1* is required for the maintenance of *Fgf10* expression during inner ear development (Zheng et al., 2003).

It is noteworthy that Shh signaling facilitates proper *Fgf10* localization during distal tip branching by inhibiting *Fgf10* expression mainly in the inter-bud regions after mesenchymal *Fgf10* expression has been initiated. However, Shh expression is also upregulated at new sites of branching, which is associated with higher levels of *Fgf10* expression. This creates an apparent paradox as to how *Fgf10* expression could be maintained in the presence of high levels of Shh expression (Chuang and McMahon, 2003). Based on our data about the *Six1* expression pattern, which co-expresses with *Fgf10* near the distal epithelium and inhibits the activity of Shh signaling in distal epithelium, wherein Six1 is also expressed (Figs.1B,C,H–

J, 10), we now propose a model in which *Six1* is a potential key regulator/coordinator of Shh/Fgf10 expression pattern and activity during lung branching. We propose that *Six1* focally expressed in distal mesenchyme inhibits Ptc1 receptor expression and thus maintains focal *Fgf10* expression by inhibiting local Shh activity. The response of distal tip epithelial cells to Fgf10 is further proposed to be facilitated because epithelial *Six1* is also potentially necessary to inhibit Shh expression and/or autocrine activity in these cells. Indeed, Shh has been shown recently to exhibit autocrine functions during the organogenesis of multiple organs (McGlinn and Tabin, 2006; Yang et al., 2008; Handrigan and Richman, 2009) and Shh autocrine activities in the lung epithelium are under investigation. Whether *Six1* controls other coordinators of Shh-Fgf10 signaling such as Hedgehog-binding protein (Hhip), BMP4 and Fgf9 will be the subjects of future study.

The role of *Six1* in epithelial progenitor cell self-renewal and cell fate determination in the lung

The lung contains different specialized epithelial cell types organized along the proximodistal axis. Yet little is known about the mechanisms that control epithelial progenitor cell self-renewal and cell fate determination in the lung. Most recently, we have shown that Eya1, which is transcriptional coactivator for Six1 during embryogenesis (Zou et al., 2004; Schlosser et al., 2008; Jemc and Rebay, 2007), is required for controlling the balance between epithelial progenitor self-renewal and differentiation in the embryonic lung (El-Hashash et al., 2011). The current study suggests that Six1 is likely to play a similar role in the self-renewal and determination of epithelial progenitor cell fate, based on its expression in distal lung epithelial cell populations that contain progenitor cells (Okubo et al., 2005; Rawlins et al., 2009) and decreased epithelial progenitors but increased epithelial differentiation after interfering with Six1 function in vivo or in vitro (Figs. 1,4–7). Indeed, *Six1* and *Eya1* genes play critical roles in the proper expression of neuronal determination and differentiation genes in the olfactory, otic and epibranchial placodes (Zou et al., 2004; Friedman et al., 2005; Bricaud and Collazo, 2006; Ikeda et al., 2007) as well as in the proliferation and survival of sensory and neuronal progenitors (Li et al., 2003; Zheng et al., 2003; Bricaud and Collazo, 2006; Zou et al., 2006b; Kriebel et al., 2007). In addition, *Six1* promotes cell fate of murine pre-placodal ectoderm and inner ear hair cells as well as leach ectodermal teloblast cells (Brugmann et al., 2004; Bricaud and Collazo, 2006 Quigley et al., 2010).

Six1 and pulmonary vascular smooth muscle cell (VSMC) development

Most recently, it has been shown that *Six1* is essential for smooth muscle cell formation in other branching organs, e.g. kidney (Nie et al., 2010). Herein we have extended these observations to the embryonic lung to demonstrate that *Six1* is critical for controlling late development of smooth muscle as it differentiates from the mesenchyme because $Six1^{-/-}$ embryos show reduced expression of vascular α-SMA in pulmonary VSMCs. Nonetheless, the undetectable expression level of Six1 in pulmonary VSMCs (data not shown) suggests several possibilities as to its actions in the regulation of VSMC development. First, *Six1* may be necessary for the expression of other auto- or paracrine factors in epithelial or mesenchymal cell lineages required for VSMC differentiation/growth. For instance, *Six1* deletion causes downregulation of the expression levels of *Fgf10* (Fig. 10L), which regulates the growth of aortic VSMC in vitro (Onda et al., 2003). A second possible mechanism is that loss of *Six1* could result in defective differentiation of VSMCs, which could lead to degradation of the smooth muscle component of the vessel wall. Interestingly, the pulmonary vascular defects of $Six1^{-/-}$ embryos seem less likely to be directly linked to lung hypoplasia because other mouse models that have severe lung hypoplasia, e.g. $Fgf9^{-/-}$ mice, exhibit normal vascular development (Colvin et al., 2001). Conversely, *Six1* is likely to play a role during the early events of pulmonary VSMC differentiation, because *Six1* expression

levels decrease during late gestation in the lung after E18.5 (Fig. 1A). Since *Eya1* deletion has similar effects on pulmonary VSMCs (El-Hashash et al., 2011), we therefore propose that the pathway of Six1-Eya1, which are expressed together in the most distal mesenchyme, may initiate a mesenchymal differentiation program that propagates from the distal to proximal regions as the lung grows, resulting in the proper differentiation of vascular smooth muscle, which occurs reciprocally to distal-proximal progression of mesenchymal differentiation.

In conclusion, the novel data presented herein provide evidence that *Six1* is important for the co-ordination of the Shh-Fgf10 signaling pathway, which regulates and coordinates key interlocking aspects of epithelial branching and both mesenchymal and vascular development during embryonic lung organogenesis.

Supplementary Material

Refer to Web version on PubMed Central for supplementary material.

Acknowledgments

We thank C. Wigfall for editing the manuscript, This study was funded by NIH-NHLBI P01 HL 60231, HL 44060, HL44977 and GM096195 grants to DW as well as California Institute of Regenerative Medicine (CIRM) stem cell grants to DW and AHE.

References

Abdelhak S, Kalatzis V, Heilig R, Compain S, Samson D, Vincent C, Weil D, Cruaud C, Sahly I, Leibovici M, et al. A human homologue of the *Drosophila eyes absent* gene underlies branchio-oto-renal (BOR) syndrome and identifies a novel gene family. Nature Genet. 1997; 15:157–164. [PubMed: 9020840]

Abler LL, Mansour SL, Sun X. Conditional gene inactivation reveals roles for Fgf10 and Fgfr2 in establishing a normal pattern of epithelial branching in the mouse lung. Dev Dyn. 2009; 238(8): 1999–2013. [PubMed: 19618463]

Bellusci S, Henderson R, Winnier G, Oikawa T, Hogan BL. Evidence from normal expression and targeted misexpression that bone morphogenetic protein (Bmp-4) plays a role in mouse embryonic lung morphogenesis. Development. 1996; 122(6):1693–702. [PubMed: 8674409]

Bellusci S, Grindley J, Emoto H, Itoh N, Hogan BL. Fibroblast growth factor 10 (FGF10) and branching morphogenesis in the embryonic mouse lung. Development. 1997a; 124(23):4867–78. [PubMed: 9428423]

Bellusci S, Furuta Y, Rush MG, Henderson R, Winnier G, Hogan BL. Involvement of Sonic hedgehog (Shh) in mouse embryonic lung growth and morphogenesis. Development. 1997b; 124(1):53–63. [PubMed: 9006067]

Bishop AE. Pulmonary epithelial stem cells. Cell Prolif. 2004; 37:89–96. [PubMed: 14871239]

Boers JE, Ambergen A, Thunnissen FB. Number and proliferation of basal and parabasal cells in normal airway epithelium. Am J Respir Crit Care Med. 1998; 157:2000. [PubMed: 9620938]

Boers JE, Ambergen A, Thunnissen FB. Number and proliferation of clara cells in normal human airway epithelium. Am J Respir Crit Care Med. 1999; 159:1585. [PubMed: 10228131]

Bricaud O, Collazo A. The transcription factor six1 inhibits neuronal and promotes hair cell fate in the developing zebrafish (Danio rerio) inner ear. J Neurosci. 2006; 26(41):10438–51. [PubMed: 17035528]

Brugmann SA, Pandur PD, Kenyon KL, Pignoni F, Moody SA. Six1 promotes a placodal fate within the lateral neurogenic ectoderm by functioning as both a transcriptional activator and repressor. Development. 2004; 131(23):5871–81. [PubMed: 15525662]

Cardoso WV. Lung morphogenesis revisited: old facts, current ideas. Dev Dyn. 2000; 219(2):121–30. [PubMed: 11002333]

Cardoso WV, Lü J. Regulation of early lung morphogenesis: questions, facts and controversies. Development. 2006; 133(9):1611–24. [PubMed: 16613830]

Carraro G, El-Hashash A, Guidolin D, Tiozzo C, Turcatel G, Young B, De Langhe S, Bellusci S, Shi W, Parnigotto PP, et al. miR-17 family of microRNAs controls FGF10-mediated embryonic lung epithelial branching morphogenesis through MAPK14 and STAT3 regulation of E-Cadherin distribution. Dev Biol. 2009; 333(2):238–250. [PubMed: 19559694]

Chenn A, Walsh CA. Regulation of cerebral cortical size by control of cell cycle exit in neural precursors. Science. 2002; 297:365–369. [PubMed: 12130776]

Chuang PT, McMahon AP. Branching morphogenesis of the lung: new molecular insights into an old problem. Trends Cell Biol. 2003; 13(2):86–91. [PubMed: 12559759]

Chuang PT, Kawcak T, McMahon AP. Feedback control of mammalian Hedgehog signaling by the Hedgehog-binding protein, Hip1, modulates Fgf signaling during branching morphogenesis of the lung. Genes Dev. 2003; 17:342–347. [PubMed: 12569124]

Coletta RD, Christensen K, Reichenberger K, Lamb J, Micomonaco D, Wolf D, Müller-Tidow C, Golub T, Kawakami K, Ford HL. The Six1 homeoprotein stimulates tumorigenesis by reactivation of cyclin A1. Proc Natl Acad Sci U S A. 2004; 101(17):6478–83. [PubMed: 15123840]

Colman H, Giannini C, Huang L, Gonzalez J, Hess K, Bruner J, Fuller G, Langford L, Pelloski C, Aaron J, Burger P, Aldape K. Assessment and prognostic significance of mitotic index using the mitosis marker phospho-histone H3 in low and intermediate-grade infiltrating astrocytomas. Am J Surg Pathol. 2006; 30(5):657–64. [PubMed: 16699322]

Colvin JS, White AC, Pratt SJ, Ornitz DM. Lung hypoplasia and neonatal death in Fgf9-null mice identify this gene as an essential regulator of lung mesenchyme. Development. 2001; 128:2095–2106. [PubMed: 11493531]

De Langhe SP, Carraro G, Warburton D, Hajihosseini M, Bellusci S. Levels of mesenchymal FGFR2 signaling modulate smooth muscle progenitor cell commitment in the lung. Dev Biol. 2006; 299:52–62. [PubMed: 16989802]

De Langhe SP, Carraro G, Tefft D, Li C, Xu X, Chai Y, Minoo P, Hajihosseini MK, Drouin J, Kaartinen V, Bellusci S. Formation and differentiation of multiple mesenchymal lineages during lung development is regulated by beta-catenin signaling. PLoS One. 2008; 3(1):e1516. [PubMed: 18231602]

De Moerlooze L, Spencer-Dene B, Revest JM, Hajihosseini M, Rosewell I, Dickson C. An important role for the IIIb isoform of fibroblast growth factor receptor 2 (FGFR2) in mesenchymal-epithelial signalling during mouse organogenesis. Development. 2000; 127(3):483–92. [PubMed: 10631169]

Del Moral PM, De Langhe S, Sala F, Veltmaat J, Tefft D, Wang K, Warburton D, Bellusci S. Differential role of FGF9 on epithelium and mesenchyme in mouse embryonic lung. Dev Biol. 2006a; 293(1):77–89. [PubMed: 16494859]

Del Moral PM, Sala FG, Tefft D, Shi W, Keshet E, Bellusci S, Warburton D. VEGF-A signaling through Flk-1 is a critical facilitator of early embryonic lung epithelial to endothelial crosstalk and branching morphogenesis. Dev Biol. 2006b; 290(1):177–88. [PubMed: 16375885]

DiSalvo CV, Zhang J, Jacobberger JW. Regulation of NIH-3T3 cell G1 phase transit by serum during exponential growth. Cell Prolif. 1995; 28:511–524. [PubMed: 7578600]

El-Hashash AH, Esbrit P, Kimber SJ. PTHrP promotes murine secondary trophoblast giant cell differentiation through induction of endocycle, upregulation of giant-cell-promoting transcription factors and suppression of other trophoblast cell types. Differentiation. 2005; 73 (4):154–174. [PubMed: 15901283]

El-Hashash AH, Alam D, Turcatel G, Bellusci S, Warburton D. Eyes absent 1 (Eya1) is a critical coordinator of epithelial, mesenchymal and vascular morphogenesis in the mammalian lung. Dev Biol. 2011; 350(1):112–126. [PubMed: 21129374]

Estefania ER, Ramirez-Camacho M, Gomar A, Trinidad B, Arellano J, Verdaguer J, Vilches C. Point mutation of an Eya1-gene splice site in a patient with Oto-facio-cervical syndrome. Ann Hum Genet. 2005; 70:140–144. [PubMed: 16441263]

Ford HL, Kabingu EN, Bump E, Mutter G, Pardee AB. Abrogation of the G2 cell cycle checkpoint associated with overexpression of HSIX1: a possible mechanism of breast carcinogenesis. Proc Natl Acad Sci U S A. 1998; 95(21):12608–13. [PubMed: 9770533]

Fougerousse F, Durand M, Lopez S, Suel L, Demignon J, Thornton C, Ozaki H, Kawakami K, Barbet P, Beckmann J, Maire P. Six and Eya expression during human somitogenesis and MyoD gene family activation. J Muscle Res Cell Motil. 2002; 23:255–264. [PubMed: 12500905]

Friedman RA, Makmura L, Biesiada E, Wang X, Keithley EM. Eya1 acts upstream of Tbx1, Neurogenin 1, NeuroD and the neurotrophins BDNF and NT-3 during inner ear development. Mech Dev. 2005; 122(5):625–34. [PubMed: 15817220]

Giangreco A, Shen H, Reynolds SD, Stripp BR. Molecular phenotype of airway side population cells. Am J Physiol Lung Cell Mol Physiol. 2004:L624–L630. [PubMed: 12909587]

Gontan C, de Munck A, Vermeij M, Grosveld F, Tibboel D, Rottier R. Sox2 is important for two crucial processes in lung development: branching morphogenesis and epithelial cell differentiation. Dev Biol. 2008; 317(1):296–309. [PubMed: 18374910]

Grifone R, Laclef C, Spitz F, Lopez S, Demignon J, Guidotti JE, Kawakami K, Xu PX, Kelly R, Petrof BJ, Daegelen D, Concordet JP, Maire P. Six1 and Eya1 expression can reprogram adult muscle from the slow-twitch phenotype into the fast-twitch phenotype. Mol Cell Biol. 2004; 24(14):6253–67. [PubMed: 15226428]

Grindley JC, Bellusci S, Perkins D, Hogan BL. Evidence for the involvement of the Gli gene family in embryonic mouse lung development. Dev Biol. 1997; 188(2):337–348. [PubMed: 9268579]

Handrigan GR, Richman JM. Autocrine and paracrine Shh signaling are necessary for tooth morphogenesis, but not tooth replacement in snakes and lizards (Squamata). Dev Biol. 2010; 337:171–186. [PubMed: 19850027]

Hogan BL, Yingling JM. Epithelial/mesenchymal interactions and branching morphogenesis of the lung. Curr Opin Genet Dev. 1998; 8:481–486. [PubMed: 9729726]

Hong KU, Reynolds SD, Giangreco A, Hurley CM, Stripp BR. Clara cell secretory proteinexpressing cells of the airway neuroepithelial body micro-environment include label-retaining 33 subset and are critical for epithelial renewal after progenitor depletion. Amer J Respir Cell Mol Biol. 2001; 24:671–681. [PubMed: 11415931]

Hoskins BE, Cramer CH, Silvius D, Zou D, Raymond RM, Orten DJ, Kimberling WJ, Smith RJ, Weil D, Petit C, Otto EA, Xu PX, Hildebrandt F. Transcription factor SIX5 is mutated in patients with branchio-oto-renal syndrome. Am J Hum Genet. 2007; 80(4):800–4. [PubMed: 17357085]

Hyatt BA, Shangguan X, Shannon JM. BMP4 modulates fibroblast growth factor-mediated induction of proximal and distal lung differentiation in mouse embryonic tracheal epithelium in mesenchyme-free culture. Dev Dyn. 2002; 225(2):153–65. [PubMed: 12242715]

Ikeda K, Ookawara S, Sato S, Ando Z, Kageyama R, Kawakami K. Six1 is essential for early neurogenesis in the development of olfactory epithelium. Dev Biol. 2007; 311(1):53–68. [PubMed: 17880938]

Jemc J, Rebay I. The eyes absent family of phosphotyrosine phosphatases: properties and roles in developmental regulation of transcription. Annu Rev Biochem. 2007; 76:513–38. [PubMed: 17341163]

Kawakami K, Sato S, Ozaki H, Ikeda K. Six family genes–structure and function as transcription factors and their roles in development. Bioessays. 2000; 22:616–626. [PubMed: 10878574]

Kelly RG, Brown NA, Buckingham ME. The arterial pole of the mouse heart forms from Fgf10-expressing cells in pharyngeal mesoderm. Dev Cell. 2001; 1(3):435–40. [PubMed: 11702954]

Kriebel M, Muller F, Hollemann T. Xeya3 regulates survival and proliferation of neural progenitor cells within the anterior neural plate of *Xenopus* embryos. Dev Dyn. 2007; 236:1526–1534. [PubMed: 17477401]

Krug P, Morinière V, Marlin S, Koubi V, Gabriel HD, Colin E, Bonneau D, Salomon R, Antignac C, Heidet L. Mutation screening of the EYA1, SIX1 and SIX5 genes in a large cohort of patients harboring branchio-oto-renal syndrome calls into question the pathogenic role of SIX5 mutations. Hum Mutat. 2010 (in press).

Kumar JP. The sine oculis homeobox (SIX) family of transcription factors as regulators of development and disease. Cell Mol Life Sci. 2009; 66:565–583. [PubMed: 18989625]

Laclef C, Hamard G, Demignon J, Souil E, Houbron C, Maire P. Altered myogenesis in *Six1* deficient mice. Development. 2003; 130:2239–2252. [PubMed: 12668636]

Lees C, Howie S, Sartor RB, Satsangi J. The hedgehog signalling pathway in the gastrointestinal tract: implications for development, homeostasis, and disease. Gastroenterology. 2005; 129(5):1696–1710. [PubMed: 16285967]

Li C, Hu L, Xiao J, Chen H, Li JT, Bellusci S, Delanghe S, Minoo P. Wnt5a regulates Shh and Fgf10 signaling during lung development. Dev Biol. 2005; 287(1):86–97. [PubMed: 16169547]

Li X, Oghi K, Zhang J, Krones A, Bush K, Glass C, Nigam S, Aggarwal A, Maas R, Rose D, Rosenfeld MG. Eya protein phosphatase activity regulates Six1-Dach-Eya transcriptional effects in mammalian organogenesis. Nature. 2003; 426(6964):238–9. [PubMed: 14628032]

Litingtung Y, Lei L, Westphal H, Chiang C. Sonic hedgehog is essential to foregut development. Nat Genet. 1998; 20:58–61. [PubMed: 9731532]

Liu Y, Hogan BL. Differential gene expression in the distal tip endoderm of the embryonic mouse lung. Gene Expr Patterns. 2002; 2(3–4):229–33. [PubMed: 12617806]

Low RB, White SL. Lung smooth muscle differentiation. Int J Biochem Cell Biol. 1998; 30:869–883. [PubMed: 9744079]

Madison BB, Braunstein K, Kuizon E, Portman K, Qiao XT, Gumucio DL. Epithelial hedgehog signals pattern the intestinal crypt-villus axis. Development. 2005; 132(2):279–289. [PubMed: 15590741]

Mailleux AA, Kelly R, Veltmaat JM, De Langhe S, Zaffran S, Thiery J, Bellusci S. Fgf10 expression identifies parabronchial smooth muscle cell progenitors and is required for their entry into the smooth muscle cell lineage. Development. 2005; 132(9):2157–66. [PubMed: 15800000]

McGlinn E, Tabin CJ. Mechanistic insight into how Shh patterns the vertebrate limb. Curr Opin Genet Dev. 2006; 16:426–432. [PubMed: 16806898]

Metzger RJ, Klein OD, Martin GR, Kransow MA. The branching programme of mouse lung development. Nature. 2008; 453(7196):745–50. [PubMed: 18463632]

Mitchell JJ, Reynolds S, Leslie K, Low R, Woodcock-Mitchell J. Smooth muscle cell markers in developing rat lung. Am J Respir Cell Mol Biol. 1990; 3:515–523. [PubMed: 2252578]

Morrisey EE, Hogan BL. Preparing for the first breath: genetic and cellular mechanisms in lung development. Dev Cell. 2010; 18(1):8–23. [PubMed: 20152174]

Nie X, Sun J, Gordon RE, Cai CL, Xu PX. SIX1 acts synergistically with TBX18 in mediating ureteral smooth muscle formation. Development. 2010; 137(5):755–65. [PubMed: 20110314]

Nyeng P, Norgaard GA, Kobberup S, Jensen J. FGF10 maintains distal lung bud epithelium and excessive signaling leads to progenitor state arrest, distalization, and goblet cell metaplasia. BMC Dev Biol. 2008; 10(8):2. [PubMed: 18186922]

Okubo T, Knoepfler P, Eisenman R, Hogan BL. Nmyc plays an essential role during lung development as a dosage-sensitive regulator of progenitor cell proliferation and differentiation. Development. 2005; 132(6):1363–74. [PubMed: 15716345]

Onda M, Naito Z, Wang R, Fujii T, Kawahara K, Ishiwata T, Sugisaki Y. Expression of keratinocyte growth factor receptor (KGFR/FGFR2 IIIb) in vascular smooth muscle cells. Pathol Int. 2003; 53(3):127–32. [PubMed: 12608893]

Pan J, Yeger H, Cutz E. Neuronal developmental marker FORSE-1 identifies a putative progenitor of the pulmonary neuroendocrine cell lineage during lung development. J Histochem Cytochem. 2000; 50:1567–1578. [PubMed: 12486079]

Pepicelli CV, Lewis PM, McMahon AP. Sonic hedgehog regulates branching morphogenesis in the mammalian lung. Curr Biol. 1998; 8:1083–1086. [PubMed: 9768363]

Perl AK, Wert S, Nagy A, Lobe C, Whitsett JA. Early restriction of peripheral and proximal cell lineages during formation of the lung. Proc Natl Acad Sci U S A. 2002; 99(16):10482–7. [PubMed: 12145322]

Pignoni F, Hu B, Zavitz K, Xiao J, Garrity P, Zipursky SL. The eye-specification proteins So and Eya form a complex and regulate multiple steps in Drosophila eye development. Cell. 1997; 91(7):881–91. [PubMed: 9428512]

Quigley IK, Schmerer MW, Shankland M. A member of the six gene family promotes the specification of P cell fates in the O/P equivalence group of the leech Helobdella. Dev Biol. 2010; 344(1):319–30. [PubMed: 20493833]

Ramasamy SK, Mailleux A, Gupte V, Mata F, Sala F, Veltmaat J, Del Moral P, De Langhe S, Parsa S, Kelly L, et al. Fgf10 dosage is critical for the amplification of epithelial cell progenitors and for the formation of multiple mesenchymal lineages during lung development. Dev Biol. 2007; 307:237–247. [PubMed: 17560563]

Rawlins EL. Lung epithelial progenitor cells: lessons from development. Proc Am Thorac Soc. 2008; 5(6):675–81. [PubMed: 18684716]

Rawlins EL, Hogan BL. Epithelial stem cells of the lung: privileged few or opportunities for many? Development. 2006; 133(13):2455–65. [PubMed: 16735479]

Rawlins EL, Clark CP, Xue Y, Hogan BL. The Id2+ distal tip lung epithelium contains individual multipotent embryonic progenitor cells. Development. 2009; 136(22):3741–5. [PubMed: 19855016]

Rayapureddi JP, Kattamuri C, Steinmetz B, Frankfort B, Ostrin E, Mardon G, Hegde RS. Eyes absent represents a class of protein tyrosine phosphatases. Nature. 2003; 426(6964):238–9. [PubMed: 14628032]

Resnitzky D, Gossen M, Bujard H, Reed SI. Acceleration of the G1/S phase transition by expression of cyclins D1 and E with an inducible system. Mol Cell Biol. 1994; 14(3):1669–79. [PubMed: 8114703]

Reynolds SD, Giangreco A, Power JH, Stripp BR. Neuroepithelial bodies of pulmonary airways serve as a reservoir of progenitor cells capable of epithelial regeneration. Am J Pathol. 2000; 156:269–278. [PubMed: 10623675]

Ruf RG, Xu PX, Silvius D, Otto EA, Beekmann F, Muerb UT, Kumar S, Neuhaus TJ, Kemper MJ, Raymond RM Jr, et al. SIX1 mutations cause branchio-oto-renal syndrome by disruption of EYA1-SIX1-DNA complexes. Proc Natl Acad Sci U S A. 2004; 101(21):8090–5. [PubMed: 15141091]

Schlosser G, Awtry T, Brugmann S, Jensen E, Neilson K, Ruan G, Stammler A, Voelker D, Yan B, Zhang C, et al. Eya1 and Six1 promote neurogenesis in the cranial placodes in a SoxB1-dependent fashion. Dev Biol. 2008; 320(1):199–214. [PubMed: 18571637]

Suzuki Y, Ikeda K, Kawakami K. Regulatory role of Six1 in the development of taste papillae. Cell Tissue Res. 2010; 339(3):513–25. [PubMed: 20143239]

Tefft D, Lee M, Smith S, Crowe D, Bellusci S, Warburton D. mSprouty2 inhibits FGF10-activated MAP kinase by differentially binding to upstream target proteins. Am J Physiol Lung Cell Mol Physiol. 2002; 283(4):L700–6. [PubMed: 12225946]

Tefft D, De Langhe S, Del Moral P, Sala F, Shi W, Bellusci S, Warburton D. A novel function for the protein tyrosine phosphatase Shp2 during lung branching morphogenesis. Dev Biol. 2005; 282(2): 422–31. [PubMed: 15950607]

Treisman JE. A conserved blueprint for the eye? Bioessays. 1999; 21(10):843–50. [PubMed: 10497334]

Urase K, Mukasa T, Igarashi H, Ishii Y, Yasugi S, Momoi MY, Momoi T. Spatial expression of Sonic hedgehog in the lung epithelium during branching morphogenesis. Biochem Biophys Res Commun. 1996; 225(1):161–6. [PubMed: 8769111]

Warburton D. Developmental biology: Order in the lung. Nature. 2008; 453(7196):73–5.

Warburton D, Schwarz M, Tefft D, Flores-Delgado G, Anderson K, Cardoso WV. The molecular basis of lung morphogenesis. Mech Dev. 2000; 92(1):55–81. [PubMed: 10704888]

Warburton D, Bellusci S, De Langhe S, Del Moral P, Fleury V, Mailleux A, Tefft D, Unbekandt M, Wang K, Shi W. Molecular mechanisms of early lung specification and branching morphogenesis. Pediatr Res. 2005; 57(5 Pt 2):26R–37R.

Warburton D, Gauldie J, Bellusci S, Shi W. Lung development and susceptibility to chronic obstructive pulmonary disease. Proc Am Thorac Soc. 2006; 3:668–672. [PubMed: 17065371]

Warburton D, Perin L, Defilippo R, Bellusci S, Shi W, Driscoll B. Stem/progenitor cells in lung development, injury repair, and regeneration. Proc Am Thorac Soc. 2008; 5(6):703–6. [PubMed: 18684721]

Warburton D, El-Hashash A, Carraro G, Tiozzo C, Sala F, Rogers O, De Langhe S, Kemp PJ, Riccardi D, Torday J, et al. Lung organogenesis. Curr Top Dev Biol. 2010; 90:73–158. [PubMed: 20691848]

Wawersik S, Maas RL. Vertebrate eye development as modeled in. Drosophila Hum Mol Genet. 2000; 9(6):917–25.

Weaver M, Dunn NR, Hogan BL. Bmp4 and Fgf10 play opposing roles during lung bud morphogenesis. Development. 2000; 127(12):2695–704. [PubMed: 10821767]

Weaver M, Batts L, Hogan BL. Tissue interactions pattern the mesenchyme of the embryonic mouse lung. Dev Biol. 2003; 258(1):169–84. [PubMed: 12781691]

White AC, Lavine KJ, Ornitz DM. FGF9 and SHH regulate mesenchymal Vegfa expression and development of the pulmonary capillary network. Development. 2007; 134(20):3743–52. [PubMed: 17881491]

Xiong W, Dabbouseh N, Rebay I. Interactions with the abelson tyrosine kinase reveal compartmentalization of eyes absent function between nucleus and cytoplasm. Dev Cell. 2009; 16(2):271–9. [PubMed: 19217428]

Xu PX, Woo I, Her H, Beier D, Maas RL. Mouse Eya homologues of the *Drosophila* eyes absent gene require Pax6 for expression in lens and nasal placode. Development. 1997a; 124(1):219–31. [PubMed: 9006082]

Xu PX, Cheng J, Epstein J, Maas RL. Mouse Eya genes are expressed during limb tendon development and encode a transcriptional activation function. Proc Natl Acad Sci U S A. 1997b; 94:11974–9. [PubMed: 9342347]

Xu PX, Adams J, Peters H, Brown M, Heaney S, Maas R. Eya1-deficient mice lack ears and kidneys and show abnormal apoptosis of organ primordia. Nat Genet. 1999; 23(1):113–7. [PubMed: 10471511]

Xu PX, Zheng W, Laclef C, Maire P, Maas R, Peters H, Xu X. Eya1 is required for the morphogenesis of mammalian thymus, parathyroid and thyroid. Development. 2002; 129(13):3033–44. [PubMed: 12070080]

Xu PX, Zheng W, Huang L, Maire P, Laclef C, Silvius D. Six1 is required for the early organogenesis of mammalian kidney. Development. 2003; 130:3085–3094. [PubMed: 12783782]

Yang L, Wang Y, Mao H, Fleig S, Omenetti A, Brown KD, Sicklick JK, Li YX, Diehl AM. Sonic hedgehog is an autocrine viability factor for myofibroblastic hepatic stellate cells. J Hepatol. 2008; 48:98–106. [PubMed: 18022723]

Yao HH, Whoriskey W, Capel B. Desert Hedgehog/Patched1 signaling specifies fetal Leydig cell fate in testis organogenesis. Genes Dev. 2002; 16:1433–1440. [PubMed: 12050120]

Zheng W, Huang L, Wei Z, Silvius D, Tang B, Xu PX. The role of Six1 in mammalian auditory system development. Development. 2003; 130(17):3989–4000. [PubMed: 12874121]

Zou D, Silvius D, Fritzsch B, Xu PX. Eya1 and Six1 are essential for early steps of sensory neurogenesis in mammalian cranial placodes. Development. 2004; 131(22):5561–72. [PubMed: 15496442]

Zou D, Silvius D, Davenport J, Grifone R, Maire P, Xu PX. Patterning of the third pharyngeal pouch into thymus/parathyroid by Six and Eya1. Dev Biol. 2006a; 293(2):499–512. [PubMed: 16530750]

Zou D, Silvius D, Rodrigo-Blomqvist S, Enerbäck S, Xu PX. Eya1 regulates the growth of otic epithelium and interacts with Pax2 during the development of all sensory areas in the inner ear. Dev Biol. 2006b; 298(2):430–41. [PubMed: 16916509]

Zou D, Erickson C, Kim EH, Jin D, Fritzsch B, Xu PX. Eya1 gene dosage critically affects the development of sensory epithelia in the mammalian inner ear. Hum Mol Genet. 2008; 17(21): 3340–56. [PubMed: 18678597]

Research Highlights

- Six1 is expressed in lung distal epithelium and mesenchyme.
- *Six1*$^{-/-}$ lungs are hypoplastic with reduced branching but increased mesenchymal cellularity
- *Six1* controls both epithelial and mesenchymal cell proliferation.
- *Six1* induces epithelial progenitor cell proliferation but inhibits differentiation.
- *Six1* coordinates Shh-Fgf10 signaling during lung development

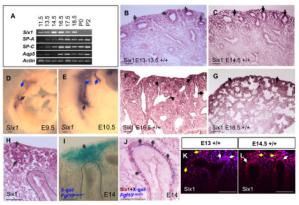

Fig. 1. Six1 expression during lung development

(A) RT-PCR shows *Six1* gene expression compared to the expression of epithelial differentiation cell markers (*SP-C*, *SP-A* and *Aqp5*). (B,C,F,G) and in situ hybridization (D,E) show strong *Six1* gene expression in lung buds (D,E; black arrows), and Six1 protein in the distal epithelial tips and distal mesenchyme (B,C,F,G; black arrows). Note *Six1* gene expression in otocysts (D; blue arrow) and pharyngeal regions (E; blue arrows). (H–I) X-gal staining of $Fgf10^{LacZ/+}$ lungs (blue; I) and Six1 immunoperoxidase staining (pink/brown; H) shows similarity in the focal expression pattern of *Fgf10* and Six1 in the distal mesenchyme (arrows). (J) Double staining of X-gal-stained $Fgf10^{LacZ/+}$lungs with Six1 antibody shows similar expression pattern between *Fgf10* and Six1 in the distal mesenchyme (arrows refer to cells that are co-stained with *Fgf10* and Six1; 5 μm section). Note that the differences in sectional planes in H–J led to differences in Six1 expression pattern in the distal epithelium compared to B,C,F,G. (K,L) Immunofluorescence staining with Six1 antibody shows nuclear expression of Six1 in most distal mesenchymal (yellow arrows) and epithelial (white arrows) cells. Blue labeling with DAPI. Scale bars: 50 μm.

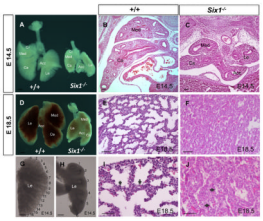

Fig. 2. Severely hypoplastic lung phenotype in *Six1*$^{-/-}$ embryos

External appearance (A,D,G,H) and histology (B,C,E,F,I,J) show severely hypoplastic *Six1*$^{-/-}$ lung phenotype at E14.5 and E18.5 compared to littermate control lungs. (B,C) *Six1*$^{-/-}$ embryos show reduced lung size at E14.5 and have fewer epithelial branches (number) than E14.5 and E12.5 control lungs (A,G,H). (F,J) low and high magnifications *Six1*$^{-/-}$ lungs at E18.5 that show greatly reduced branching, dense mesenchymal cellularity and arrested expansion of epithelial tubules compared to wildtype control littermates (E,I). Note greatly reduced primitive pre-alveoli in *Six1*$^{-/-}$ lungs (J; arrows) compared to wildtype lungs (I; arrows). (Cr) Cranial lobe, (Med) Medial lobe, (Ca) Caudal lobe, (Acc) Accessory lobe, (Le) Left lobe. Scale bars: panels A,D,G,H, 0.25 mm, panels B,C,E,F,I,J, 50 μm.

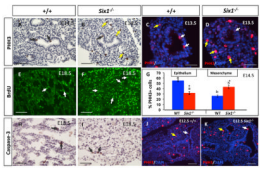

Fig. 3. Cell proliferation and apoptosis in *Six1*$^{-/-}$ lung epithelium/mesenchyme

Cell proliferation analysis by PHH3 (A–D) or BrdU (E,F) antibody staining shows increased number of proliferative cells in *Six1*$^{-/-}$ lung mesenchyme at E14.5 (B; yellow arrows), E13.5 (D; yellow arrows) and E18.5 (F; arrows) compared to corresponding wildtype littermates. Note the reduced number of proliferative PHH3-positive cells in the distal epithelium of E13.5 *Six1*$^{-/-}$ lungs compared to wildtype lungs (C,D; white arrows). This reduction is also observed in E14.5 *Six1*$^{-/-}$ lungs (B versus A; black arrows). (G) Quantification of experiments shown in A–B. *Bars carrying the same letter (a, b,) are significantly different from one another ($n = 3$; $p < 0.05$; Student's *t*-test). (H,I) Caspase-3 antibody staining shows no apparent change in apoptotic cell number (arrows) in *Six1*$^{-/-}$ lungs compared to control lungs. (J,K) Staining with PHH3 antibody shows comparable cell proliferation in the mesenchyme (yellow arrows) and epithelium (white arrows) between *Six1*$^{-/-}$ and wildtype lungs at E12.5. (A,B,E,F,H,I) counterstaining with hematoxylin. (C,D,J,K) Blue labeling with DAPI. Scale bars: 50 μm.

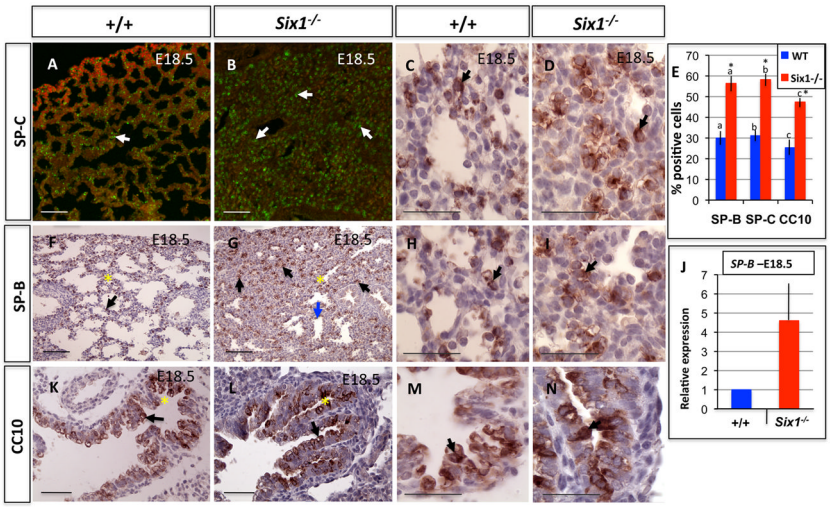

Fig. 4. Increased epithelial cell differentiation in *Six1*$^{-/-}$ lungs

(A–B,F–G,K–L) Immunohistochemistry shows increased expression of lung epithelial cell differentiation markers SP-C, SP-B and CC10 in E18.5 *Six1*$^{-/-}$ lungs (B,G,L; black arrows) compared to wildtype lungs (A,F,K; black arrows). Note that blue arrow in G refers to primitive pre-alveoli. (C,D,H,I,M,N) high magnifications show no apparent change in the expression levels of SP-C (C,D), SP-B (H,I) or CC10 (M,N) inside the cells in mutant lungs compared to control lungs (arrows). H,I,M,N represent high magnifications of the area marked with an asterisk in F,G,K,L; respectively. (E) Quantification of experiments shown in A,B,F,G,K,L for SP-C,SP-B and CC10. *Bars carrying the same letter (a, b, c) are significantly different from one another ($n = 3$; $p < 0.05$; Student's *t*-test). (J) Real-time RT-PCR shows remarkable increased expression of *SP-B* in E18.5 *Six1*$^{-/-}$ lungs. Scale bars: 50 μm.

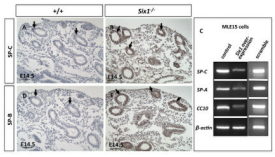

Fig. 5. Epithelial differentiation increases during pseudoglandular phase in *Six1*$^{-/-}$ lungs

(A,B,D,E) Immunoperoxidase staining shows increased expression of SP-C and SP-B in E14.5 *Six1*$^{-/-}$ lungs compared to control littermates (compare arrows in B,E with those in A,D). (C) RT-PCR shows reduced expression levels of *SP-C*, *SP-A* and *CC10* after *Six1* overexpression in MLE-15 cells for three days in culture (Scramble = control scramble oligonucleotides). Scale bars: 50 μm.

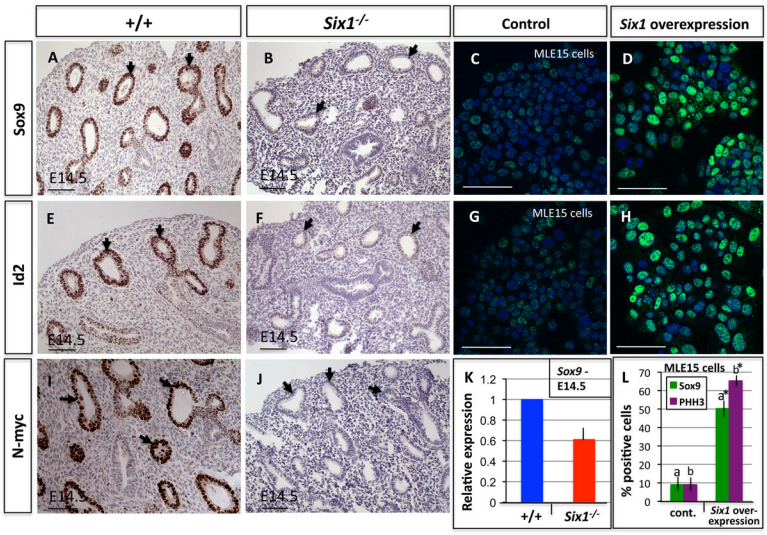

Fig. 6. Reduced expression of distal epithelial progenitor markers in *Six1*$^{-/-}$ lungs

(A,B,E,F,I,J) Immunohistochemistry shows marked reduction of the expression levels of epithelial progenitor markers Sox9, Id2 and N-myc at distal epithelial tips of E14.5 *Six1*$^{-/-}$ lungs (B,F,J; arrows), compared to control lungs (A,E,I; arrows). This decrease was also demonstrated at gene levels by real-time PCR for *Sox9* (K). (C,D,G,H) Immuno-cytochemistry shows increased number of cells that express Sox9 (D) and Id2 (H) after *Six1* overexpression in MLE-15 cells for three days in culture. Blue nuclear labeling with DAPI in C,D,G,H. (L) Quantification of experiments shown in C,D for Sox9 and for PHH-3-positive mitotic MLE15 cells. *****Significantly different from control (n=527; p< 0.05; Student's t-test). Scale bars: 50 μm.

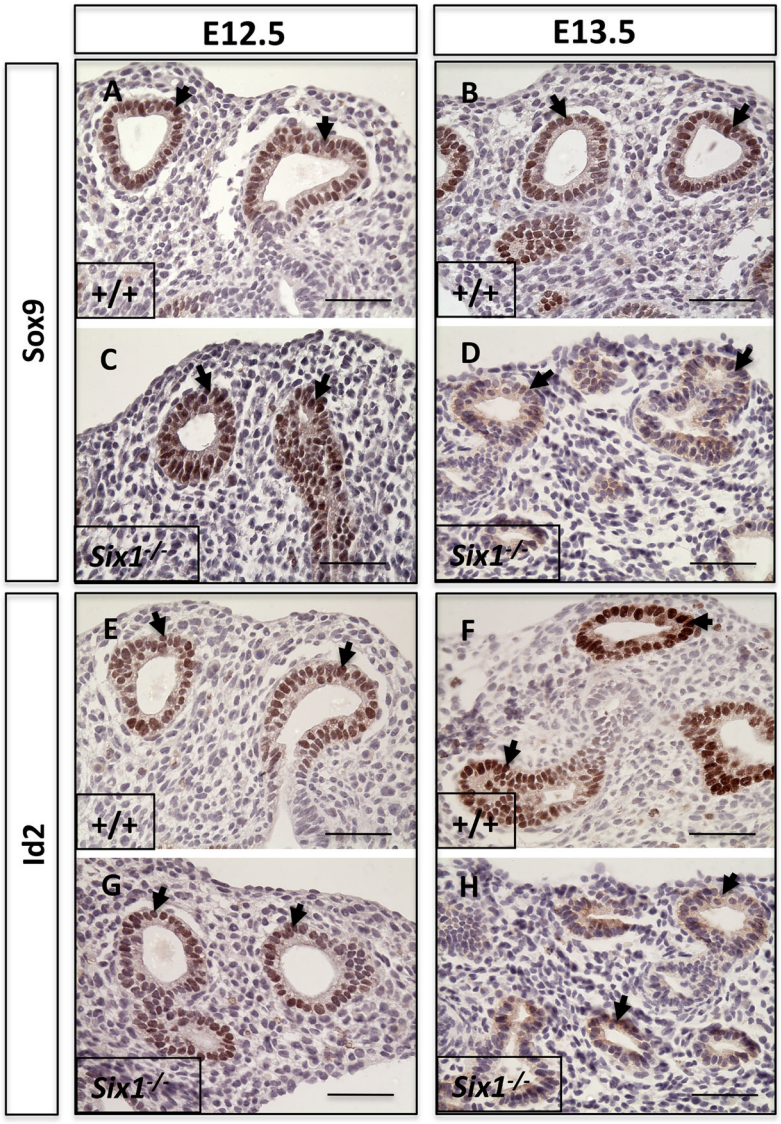

Fig. 7. Normal expression of distal epithelial progenitor markers in *Six1*$^{-/-}$ lungs before E13–13.5 of development

Immunoperoxidase staining of E12.5 *Six1*$^{-/-}$ lungs shows that the expression levels of Sox9 (C) and Id2 (G) at distal epithelial tips are comparable with control lungs (A,E; arrows). (D,H) the expression levels of Sox9 (D) and Id2 (H) reduce in mutant compared to control lungs (B,F; arrows) at E13–13.5. Scale bars: 50 μm.

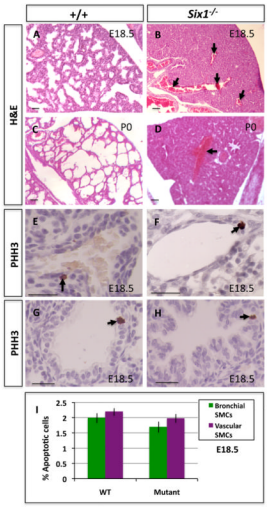

Fig. 8. *Six1*$^{-/-}$ embryos and neonates exhibit blood vessel congestions

(A–D) Haematoxylin and Eosin staining shows increased blood vessel congestion in *Six1*$^{-/-}$ lungs at E18.5 and at birth (B,D; arrows) compared to control littermates (A,C). (E–H) Immunohistochemistry with PHH3 antibody shows comparable cell proliferation between mutant and control lungs in the blood vessel walls (E,F; arrows) and bronchi (G,H, arrows). (I) Quantification of the number of caspase-3-positive cells show no significant difference in apoptosis between control and mutant lung bronchial and vascular smooth muscles (SMCs; n=200; $p< 0.05$; Student's t-test). Scale bars: 50 μm.

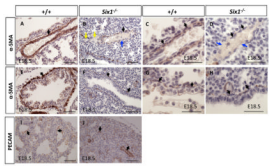

Fig. 9. Defective smooth muscle integrity in *Six1*$^{-/-}$ embryonic lungs

(A–H) Immunohistochemistry with α-SMA antibody shows severely reduced staining surrounding blood vessels (B; black arrows) and large bronchial airways (F; black arrows) in *Six1*$^{-/-}$ lungs compared to control lungs (A,E; black arrows). Note several breaches in the blood vessel walls, (B,D; blue arrows) and thin smooth muscle layer with herniation of the intact endothelial cell layer (B; yellow arrows) in mutant lungs. (C,D,G,H) α-SMA/ Haematoxylin staining shows that spindle-shaped smooth muscle cells present in *Six1*$^{-/-}$ lungs surrounding blood vessels and large bronchia (D,H; black arrows) compared to control lungs (C,G; black arrows). Note that sections are weakly stained with α-SMA antibody in order to see cell morphology in C,G. (I–J) Staining with PECAM antibody shows comparable signals in wildtype and *Six1*$^{-/-}$ lungs (I,J; black arrows). Scale bars: 50 μm.

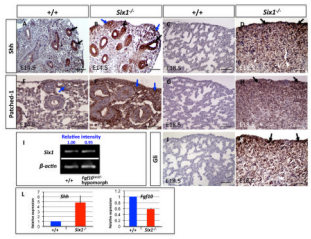

Fig. 10. Increased Shh signaling activity, but decreased *Fgf10* expression in *Six1*$^{-/-}$ lungs

(A–H,J–K) Immunohistochemistry with Shh (A–D), Patched-1 (E–H) or Gli (J–K) antibody shows increased expression levels of Shh, Patched-1 and Gli proteins (arrows) in E14.5 and E18.5 *Six1*$^{-/-}$ lungs compared to control lungs. Note increased Shh and Patched-1staining in the mesenchyme at E14.5 (B,F; blue arrows) and increased Shh expression in the epithelium at E14.5 (B; black arrows). (I) RT-PCR shows no apparent change in *Six1* expression in E14.5 *Fgf10*$^{LacZ/-}$ hypomorphic lungs. (L) Real-time PCR shows increased *Shh*, but decreased of *Fgf10* expression levels in E18–18.5 *Six1*$^{-/-}$ lungs. Scale bars: 50 μm.

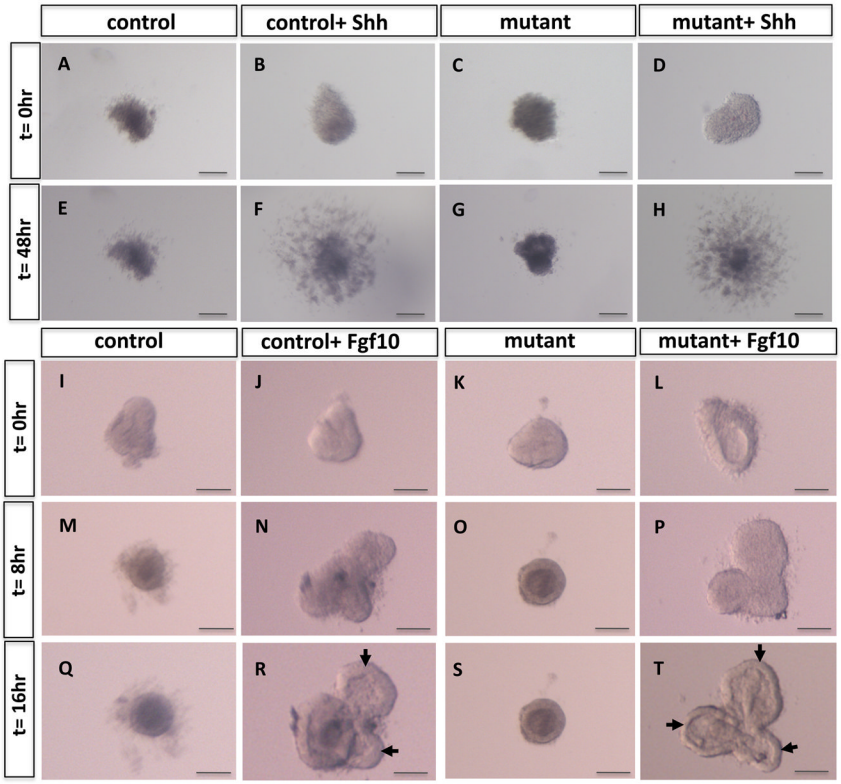

Fig. 11. Effect of exogenous Shh and Fgf10 proteins on isolated distal lung mesenchyme and epithelium; respectively

(A,E,C,G) Isolated E12.5 distal mesenchyme from either wildtype control or *Six1*$^{-/-}$ lungs grown for 48 hr in the absence of Shh protein undergo necrosis (E,G). (B,F,D,H) In the presence of recombsinant Shh protein, the mesenchymal explants of wildtype or *Six1*$^{-/-}$ lungs grow and many mesenchymal cells invading the Matrigel are observed in periphery. (I,M,Q,K,O,S) Isolated E12.5 distal epithelium from either wildtype or *Six1*$^{-/-}$ lungs grown for 16 hr in the absence of Fgf10 protein undergo necrosis (Q,S). (J,N,R,L,P,T) In the presence of recombinant Fgf10 protein, the epithelial explants of *Six1*$^{-/-}$ lungs (L,P,T) grow considerably and continued to branch forming new branching tips (arrows) similar to wildtype explants (J,N,R). Scale bar: 80 μm.

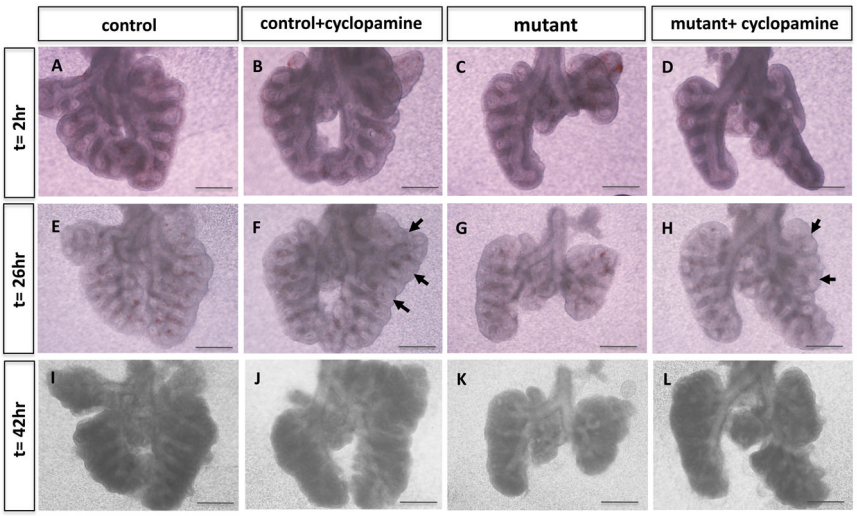

Fig. 12.

Effect of cyclopamine-mediated inhibition of the Shh pathway on *Six1*$^{-/-}$ lung growth in culture for 42 hr. (A,E,I) control E12–12.5 lungs grow and form new branches in culture in the absence of cyclopamine. (B,F,J) control E12–12.5 lungs growing in the presence of 5 μmol/l cyclopamine exhibit epithelial branching and more dilated epithelial end buds (arrows refer to dilation in F). (C,G,K) E12–12.5 *Six1*$^{-/-}$ lungs do not grow well in culture in the absence of cyclopamine. (D,H,L) E12–12.5 *Six1*$^{-/-}$ lungs growing in the presence of 5μmol/l cyclopamine exhibit increased epithelial branching and dilated epithelial end buds (arrows refer to dilation in H). Note increased lung thickness and size after 42 hr in culture (I,J,L). Scale bar: 190 μm.

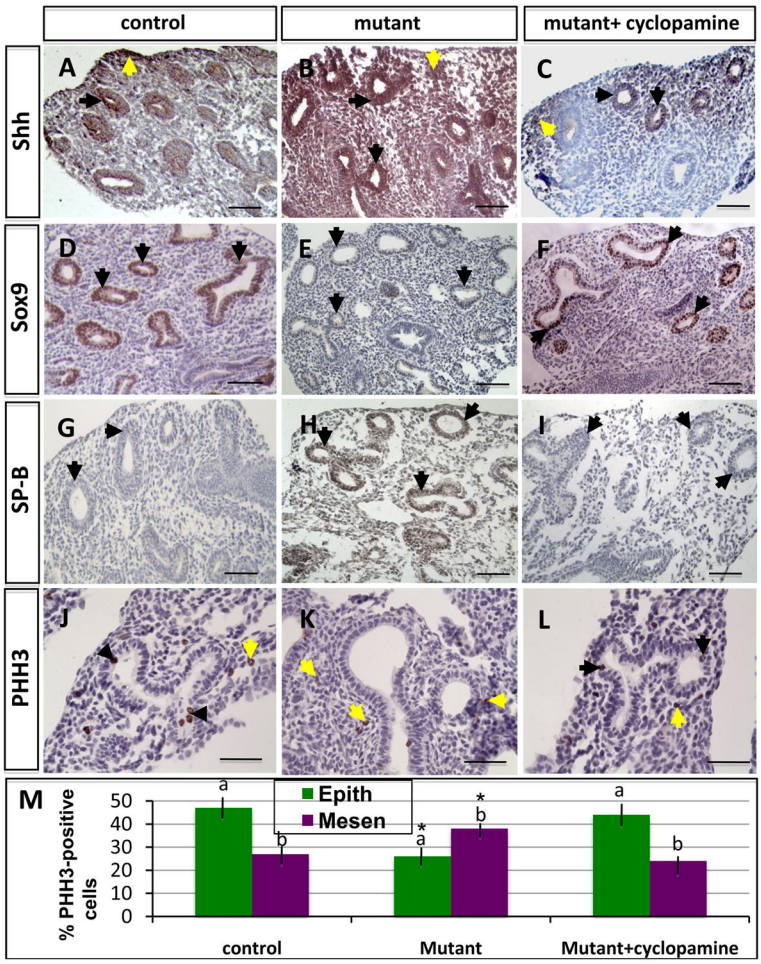

Fig. 13. Developmental changes of *Six1*$^{-/-}$ lung growing in culture for 26 hr after treatment with cyclopamine

Immunohistochemistry with specific antibodies shows increased levels of Shh (B; in the epithelium; black arrows and in the mesenchyme; yellow arrows) and SP-B (H; black arrows) as well as PHH-3 positive cells in the mesenchyme (K; yellow arrows) in *Six1*$^{-/-}$ compared to control wildtype lungs (A,G,J). (E) Decreased Sox9 expression in mutant lungs (black arrows). (C,F,I,L) Treatment of mutant lungs with cyclopamine reduces the expression of Shh (C; yellow arrows in the mesenchyme and black arrows in the epithelium) and SP-B (I; black arrows) into control lung levels, but increases Sox9 expression (F; black arrows) and PHH3-positive epithelial cells (L; black arrows). Note reduced number of PHH3-positive cells in the distal epithelial tips, but increased mitosis in the mesenchyme (yellow arrows) of mutant lungs in K. (A–L) counterstaining with Haematoxylin. (M) Quantification of the number of PHH3-positive cells for the experiment showing in J–L. *Bars carrying the same letter (a,b) are significantly different from one another (n=3; p< 0.05; ANOVA-Dunnett test). Note significant changes of mitosis of both distal epithelium and mesenchyme in mutant lungs without treatment with cyclopamine. Epith, epithelium. Mesen, mesenchyme. Scale bars: 50 μm.